

On the Phase Structure of the 3D $SU(2)$ –Higgs Model and the Electroweak Phase Transition

T. S. Evans*, H. F. Jones†, and A. Ritz‡

*Theoretical Physics Group, Blackett laboratory,
Imperial College, Prince Consort Rd., London, SW7 2BZ, UK.*

(May 13, 2019)

Abstract

The phase structure of the 3D $SU(2)$ –Higgs model, the dimensionally reduced effective theory for the electroweak model at finite temperature, is analysed on the lattice using a variant of the linear δ –expansion. We develop a systematic variational cumulant expansion for general application to the study of gauge invariant operators in 3D gauge-Higgs models, with emphasis on the symmetric phase. In particular, the technique is not restricted to finite lattice volumes, and application to the fundamental 3D $SU(2)$ –Higgs model allows the discontinuity of certain observables across the first–order transition to be observed directly for small 4D Higgs masses. The resulting phase structure agrees well with Monte Carlo simulations for small Higgs masses, but, at least to the order calculated, the technique is less sensitive to the expected evolution of the transition to a crossover for Higgs masses above 80 GeV.

PACS Numbers : 11.10.Wx, 11.15.Ha, 11.15.Tk, 64.60.-i

Typeset using REVTeX

*email: t.evans@ic.ac.uk

†email: h.f.jones@ic.ac.uk

‡email: a.ritz@ic.ac.uk

I. INTRODUCTION

Recently, considerable effort has been invested in the study of the phase structure of the electroweak model and various extensions at finite temperature. In particular, the properties of the first-order phase transition are of great cosmological significance, in order to determine whether the generation of baryon asymmetry is viable at such a transition.

The study of gauge theories, such as the electroweak model, at finite temperature is plagued by the fact that combined with the need for non-perturbative techniques to study the confining symmetric phase, infra-red effects also lead to a large effective expansion parameter in the broken phase where perturbation theory appears naively applicable. This is particularly true for moderately large Higgs masses, $m_H \sim m_W$. A considerable advance for the study of static, thermodynamic, properties has been the systematic development of dimensional reduction techniques [1] allowing the mapping, via matching of Green functions, of the full $4D$ theory onto a super-renormalizable $3D$ theory corresponding to the Matsubara zero-modes. For the electroweak theory in the transition region this procedure may be carried out perturbatively as the gauge coupling is small, while infra-red problems are also absent as such effects are encoded in the dynamics of the effective $3D$ theory. If one ignores the unimportant $U(1)$ factor [2], the effective theory is a super-renormalizable $SU(2)$ -Higgs model. This super-renormalizability, and also the non-triviality of the Higgs sector in $3D$, allow a more straightforward approach to the continuum limit than in conventional $4D$ studies [3–8]. Removal of thermally massive fermions, and smaller $3D$ lattices have allowed detailed Monte Carlo studies of the $3D$ theory, the conclusion being that the first-order transition which grows increasingly weaker as the Higgs mass increases, actually ceases to be first order and is presumably an analytic crossover for $m_H \geq 80$ GeV [9–11]. This is plausible as in this system there is no gauge invariant order parameter which can physically distinguish the two phases [12]. Indeed recent analysis of the spectrum for large Higgs masses [13,14] has indicated that the structure is very similar on both sides of the transition/crossover region. One can intuitively map three massive vector bosons and one scalar of the Higgs phase smoothly onto the three vector and one scalar bound state resonances of the confining phase. However, actual identification of the spectrum requires more care due to operator mixing and the presence of low lying excited states.

Notwithstanding the success of Monte Carlo simulations, it is also clear that many of the advantages of dimensional reduction for the study of finite temperature gauge theories are more generally applicable. Indeed, renormalization group [15,16], and Schwinger-Dyson [17], techniques were among the first to suggest loss of the first-order transition, stimulating much of the recent lattice activity. Furthermore, analysis of the spectrum, and properties of the crossover very close to the endpoint of the first-order transition line, may well prove difficult to study via Monte Carlo techniques due to the requirement for large volume lattices in order to overcome finite size effects. This is especially true if the transition line ends at a second-order endpoint.

In this paper we shall investigate the fundamental $3D$ $SU(2)$ -Higgs model on the lattice using an analytic technique which is a variant of the linear δ -expansion (LDE). The approach is developed as a systematic method applicable to the calculation of gauge invariant expectation values in gauge-Higgs theories on lattices of arbitrary (even infinite) volume. We concentrate in this instance on the fundamental $SU(2)$ -Higgs model as the dimensionally

reduced effective theory for the electroweak model and consider the calculation of average plaquette and hopping term expectation values in order to extract the phase structure. Some preliminary results of this work were presented in [18]. A similar methodology has been used previously for studying the average plaquette energy in $4D$ lattice gauge theory [19–25], the phase structure in a mixed fundamental/adjoint $SU(2)$ model [26], Higgs models [27–29], and calculation of the scalar glueball mass in pure $SU(2)$ gauge theory [30]. The results have generally agreed well with Monte Carlo data where available.

The layout of the paper is as follows. In section 2 we briefly review the relevant relations between the dimensionally reduced $3D$ theory and the electroweak $4D$ parameters, which allow us to present the results in terms of $4D$ Higgs mass and temperature variables. In Section 3 we review the LDE approach, and describe the application to gauge-Higgs systems, and the fundamental $SU(2)$ -Higgs model in particular. The calculational techniques are discussed in section 4, with more technical details relegated to two appendices. Results for relevant observables in the transition region are presented, with higher order cumulants being used to help locate the critical line precisely; the results agree remarkably well with Monte Carlo estimates. Some concluding remarks are presented in Section 5.

II. DIMENSIONAL REDUCTION OF THE ELECTROWEAK MODEL AT FINITE TEMPERATURE

A full analysis of dimensional reduction of various $4D$ theories including the standard model and MSSM, involving detailed matching of Green functions has been presented in [1]. Here we shall simply summarise the procedure and present the relations between the parameters for later use.

The reduction procedure consists of two stages. In the first, high momentum modes of the gauge field, and the thermally massive fermions are integrated out, while retaining the temporal component of the gauge field A_0 as an additional adjoint Higgs. The mass of this field is given by the Debye screening mass as $O(gT)$, and this field may also be integrated out as a second step. One then matches the resulting Green functions with those for a super-renormalizable $3D$ theory which, neglecting the $U(1)$ factor, is an $SU(2)$ -Higgs theory,

$$\mathcal{L} = \frac{1}{4}G_{ij}^a G_{ij}^a + (D_i\Phi)^\dagger(D_i\Phi) + m_3^2\Phi^\dagger\Phi + \lambda_3(\Phi^\dagger\Phi)^2, \quad (1)$$

where G_{ij}^a is the $SU(2)$ field strength, and Φ an $SU(2)$ doublet. More recently, study of the full $SU(2) \times U(1)$ theory has indicated [2] that the phase structure is not qualitatively changed, thus for convenience we consider only the case where the Weinberg angle is set to zero. It is an important feature of the Green function matching procedure that it does not introduce additional non-local terms which generically arise in a low energy effective theory obtained by explicitly integrating out massive modes, and may give dominant contributions. It has been shown [1] that the Green functions of (1) approximate those for the full theory in the infra-red up to corrections of the form $\delta G/G \sim O(g^3)$ where g is the $4D$ gauge coupling. This is an acceptable approximation as the phase transition region is expected to have a weakly coupled gauge sector.

The 3D gauge coupling g_3^2 , Higgs mass m_3^2 and self coupling λ_3 will depend on the temperature and the underlying 4D parameters. In this theory all parameters are dimensionful and one may fix the scale with the gauge coupling g_3^2 . The phase structure and 4D temperature dependence are then determined by the two dimensionless ratios [1] $x \equiv \lambda_3/g_3^2$ and $y \equiv m_3^2(g_3^2)/g_3^4$. However, the 3D theory is an effective theory for a large class of 4D theories with differing scalar and fermionic field content, and the mapping needs to be established for each individually. As discussed above, this may be performed perturbatively as calculations only involve massive modes, and are thus free of infra-red problems. For the standard model the relevant mapping has been determined in [1]. For simplicity, we consider the mapping to the effective 4D parameters m_H^* and T^* of the 4D $SU(2)$ -Higgs model [31,9] which are convenient for representing the results, and differ by only a few percent from the pole mass and temperature. Using tree-level relations [31], the temperature is given purely by the gauge coupling, $g_3^2 = 0.44015T^*$, while the dimensionless ratios are

$$x = -0.00550 + 0.12622h^2 \quad (2)$$

$$y = 0.39818 + 0.15545h^2 - 0.00190h^4 - 2.58088 \frac{(M_H^*)^2}{(T^*)^2}, \quad (3)$$

where $h = m_H^*/80.6$ GeV is a dimensionless Higgs mass. As there is this direct connection between (m_H^*, T^*) and g_3^2, x , and y we can convert analysis of the phase structure in the x, y plane to the physically more meaningful (m_H^*, T^*) variables.

Focusing now on the 3D theory, the fact that the infrared details are still encoded in the dynamics of this theory means that a non-perturbative approach is required. The super-renormalizability of (1) now ensures that one can calculate perturbatively exact RG trajectories. Only the mass parameter receives contributions at two-loop order, and there are no three- or higher-loop contributions. We adopt a lattice regularization, and the standard Wilson lattice analogue of the action (1) with lattice constant a may be written in the form

$$S = \beta \sum_p \frac{1}{2} \text{Tr} U_p + \frac{1}{2} \beta_h \sum_{l_{ij}} \rho_i \rho_j \text{Tr} U_{ij} - \sum_i \left[\rho_i^2 + \beta_r (\rho_i^2 - 1)^2 \right], \quad (4)$$

where we choose to represent the Higgs doublet in the form $\Phi = \rho_i V_i$, with $\rho \in \mathbf{R}_+$ and V an element of the fundamental representation of $SU(2)$. We then make a gauge transformation $U_{ij} \rightarrow V_i U_{ij} V_j^\dagger$ to rotate the phase of the Higgs field in the interaction term to the identity at each site. Thus the interaction term becomes $\rho_i \rho_j \text{Tr} U_{ij}$. While this choice may not appear desirable in the symmetric phase, it is advantageous for calculational purposes, and in previous lattice studies [27] has led to good results, so we shall also adopt it here. In the continuum limit, which may be determined by the RG trajectory noted above, the dimensionless parameters β, β_h, β_r are related to the parameters of the continuum theory as follows [31]:

$$x = \frac{\beta \lambda}{\beta_h^2} \quad g_3^2 a = -\frac{4}{\beta} \quad (5)$$

$$y = \frac{\beta^2}{8} \left(\frac{1}{\beta_h} - 3 - \frac{2\beta_r}{\beta_h} \right) + \frac{3\Sigma\beta}{32\pi} (1 + 4x) \\ + \frac{1}{16\pi^2} \left[\left(\frac{51}{16} + 9x - 12x^2 \right) \left(\ln \frac{3\beta}{2} + \zeta \right) + 5.0 + 5.2x \right], \quad (6)$$

where $\Sigma = 3.17591$ and $\zeta = 0.09$ follow from perturbative analyses. For different values of the lattice constant a these relations define a constant physics curve, or RG trajectory, for fixed g_3^2, x, y in the space β, β_h, β_r .

With the preceding results, we may now analyse the phase structure of the lattice $SU(2)$ -Higgs model in $3D$ and subsequently convert the results back to physical parameters. The details of this procedure will be discussed in Section 4, while in the next section we review details of the LDE, and discuss its application to the $SU(2)$ -Higgs model.

III. LDE ANALYSIS OF THE $SU(2)$ -HIGGS MODEL

The linear δ -expansion is an analytic approach to calculations in field theory which makes use of an artificial expansion not dependent on the existence of small coupling constant for its validity. Nonetheless, calculations are generally no more complex than standard perturbative Feynman diagrams. An essential feature of this approach is the ability to optimize convergence of the series by fixing additional parameters appearing in the extended action.

The LDE action has the form

$$S_\delta = (1 - \delta)S_0(J) + \delta S, \quad (7)$$

where S_0 contains some dependence on a variational parameter J , and $S_\delta \rightarrow S$ the theory under consideration, independent of J , when $\delta = 1$. The generating functional for Green functions may then be expanded to an appropriate order in δ , which is then set to unity.

As the power series is only calculated to a finite order, it retains some dependence on J which would be absent in a full summation. A well motivated criterion for fixing J is the principle of minimal sensitivity (PMS) [32], whereby J is chosen at a local extremum of a physical quantity. i.e. if $X_N(J)$ denotes the N 'th approximation to X , then we impose

$$\frac{\partial X_N(J)}{\partial J} = 0. \quad (8)$$

This or a similar criterion is intrinsic to the success of the LDE, providing the nonperturbative dependence on the coupling constant, and has been shown to induce convergence of the series in 0- and 1-D field theories [33,34] where the perturbative series are asymptotic and eventually diverge factorially.

The technique has also been applied with success to lattice gauge theories, where different choices of S_0 are appropriate in the weak and strong coupling regimes. In the strong coupling regime an approach using a maximal tree of plaquettes [21,24] has proved successful in describing the strong coupling behaviour of the average plaquette energy E_P . The weak coupling regime has also been considered using a quadratic S_0 [22,23] and using a single link S_0 in [19]. These techniques have since been applied at finite temperature [20], to the $SU(2)$ mass gap [30], mixed $SU(2) - SO(3)$ phase structure [26], and also to lattice Higgs models in [27-29].

In the present context, the variational cumulant expansion approach using a single link S_0 seems most appropriate. At this stage we retain the full gauge Higgs coupling and choose a background action of the form (cf. (4))

$$S_0 = \sum_l (J + \beta_h \rho_i \rho_j) \frac{1}{2} \text{Tr} U_l - \sum_i [\rho_i^2 + \beta_r (\rho_i^2 - 1)^2], \quad (9)$$

thereby introducing a variational parameter J . It should be noted that this background is not explicitly gauge invariant due to the single link action. In the present context this is not of concern since we shall only calculate the expectation value of gauge invariant operators. However, if one were to calculate gauge non-invariant expectations the correct approach [20] is to note that a priori J is link dependent and may have an arbitrary $SU(2)$ phase which should be summed over. Once this procedure is carried out one finds that gauge non-invariant expectation values vanish as expected¹. Using the methodology just described we evaluate expectation values as follows:

$$\langle X \rangle = \frac{1}{Z} \int [dU][d\rho] X e^{\delta(S-S_0)} e^{S_0}, \quad (10)$$

where the partition function is given by

$$Z = e^{-W} = \int [dU][d\rho] e^{\delta(S-S_0)} e^{S_0}, \quad (11)$$

in which $[dU]$ denotes the standard Haar measure over $SU(2)$, and $[d\rho] = \prod_i d\rho_i \rho_i^3$. An N^{th} order approximant to $\langle X \rangle$ in the LDE then takes the form,

$$\langle X \rangle_N = \sum_{n=0}^N \frac{\delta^n}{n!} \langle X(S-S_0)^n \rangle_C, \quad (12)$$

where $\langle X \rangle_C$ denotes the connected expectation value, or cumulant, of X in the S_0 background. e.g. $\langle AB \rangle_C = \langle AB \rangle_0 - \langle A \rangle_0 \langle B \rangle_0$. It is the expansion of the partition function in the denominator of the expectation value to the appropriate order in δ that naturally subtracts the disconnected components. This is crucial, as one now observes that the physical expectation value reduces to a sum of connected expectation values for which one can introduce a convenient diagrammatic notation in order to keep track of the independent contributions. Furthermore, connectedness implies that one can effectively take the lattice volume to infinity as at any finite order only a finite number of distinct diagrams will contribute. Summing all such diagrams over an infinite lattice will then simply lead to coefficients proportional to the number of sites N in the lattice, and thus expectation values normalised as $\langle X \rangle / N$ will be finite and calculable, independent of the finiteness or otherwise of N .

Therefore, for practical purposes the calculation reduces to the enumeration and calculation of expectation values of connected diagrams in the S_0 background, i.e. we require²

¹It is interesting to note that this approach does in principle allow the possibility of considering gauge fixed operators, and this may be of interest in comparing gauge invariant lattice results for the spectrum with gauge fixed perturbative calculations [35–37].

²Note that if convenient one may reduce the number of diagrams required by calculating $\langle X(S^n) \rangle_0$ in an $S_0(1-\delta)$ background, and then subsequently expand the result to the appropriate order in δ .

$$\langle X \rangle_0 = \frac{1}{Z_0} \int [dU][d\rho] X e^{S_0}, \quad (13)$$

with

$$Z_0 = \int [dU][d\rho] e^{S_0}, \quad (14)$$

Actual calculations are simplified by recognising that the terms in the $SU(2)$ -Higgs action involve only real constants, the ρ_i , or $SU(2)$ characters since $\text{Tr}U = \chi_{1/2}(U)$ for U an element of the fundamental representation of $SU(2)$. The free action S_0 also consists only of constant factors and fundamental $SU(2)$ characters. For example, the S_0 partition function takes the form,

$$Z_0 = \int \left[\prod_i d\rho_i \rho_i^3 \right] \int \left[\prod_{ij} dU_{ij} \exp \left(\sum_l (J + \beta_h \rho_i \rho_j) \chi_{1/2}(U_{ij}) - \sum_i V_H(\beta_r, \rho_i) \right) \right], \quad (15)$$

where $V_H = \rho^2 + \beta_r(\rho^2 - 1)^2$ is the Higgs potential. The expectation value integrals are most easily evaluated making use of a character expansion for the exponentiated S_0 . For the fundamental representation of $SU(2)$ we have (see e.g. [38])

$$e^{\frac{1}{2}J\chi_{1/2}(U)} = \frac{2}{J} \sum_{r=0} (r+1) I_{r+1}(J) \chi_{r/2}(U), \quad (16)$$

where we have made use of the relation $I_p(x) - I_{p+2}(x) = 2(p+1)I_{p+1}(x)/x$ for modified Bessel functions. Then via use of the orthogonality relation for characters the group integration becomes trivial. In certain higher order cases expectation values do not reduce to simple products of link characters and a rather more general technique is then required (see Appendix A for more details). In order to make the calculations tractable we will make the assumption that the Higgs modulus varies relatively slowly over the lattice. More precisely, we assume that $\rho_i \rho_j = \rho_i^2 + \delta^2 \rho_i \Delta \rho_i$, where $\Delta \rho_i = \rho_j - \rho_i$ with i and j nearest neighbour sites. This is motivated by the success of the approach, ignoring the correction altogether, in spin-glass systems [39], which are very similar to the $\beta \rightarrow 0$ limit of the $SU(2)$ -Higgs lattice theory. The validity of this assumption for large β is less clear. However, given our ansatz, at higher order in δ the correction terms enter in the calculation in a self-consistent way. Consequently, up to $O(\delta^2)$, once the group integration has been performed via character expansion techniques, the remaining integrals over the modulus of the Higgs field generically take the form (for each link)

$$A_r^n \equiv \left[\int_0^\infty d\rho \rho^{2n+3} e^{-V_H} \left((r+1) \frac{I_{r+1}(J + \beta_h \rho^2)}{\frac{1}{2}(J + \beta_h \rho^2)} \right)^d \right]^{1/d}, \quad (17)$$

which may be calculated numerically (see Appendix B for an analytical study, and an expansion in β_h). All the required expectation values may then be expressed in terms of the ratios $B_r^n \equiv A_r^n / A_0^n$.

IV. EXPECTATION VALUE CALCULATIONS AND THE PHASE STRUCTURE

In considering expectation values it is convenient to introduce a graphical notation for the standard operators appearing in the action. We define:

$$\square = \sum_p \frac{1}{2} \text{Tr} U_p \quad (18)$$

$$\bullet\text{---}\bullet = \sum_l \frac{1}{2} \rho_i \rho_j \text{Tr} U_{ij} \quad (19)$$

$$\text{---} = \sum_l \frac{1}{2} \text{Tr} U_l. \quad (20)$$

The gauge invariant quasi-order parameters, the average plaquette, and the hopping term, may then be conveniently represented in the form

$$\langle E_P \rangle = \frac{1}{N_p} \langle \square \rangle \quad (21)$$

$$\langle E_L \rangle = \frac{1}{N_l} \langle \bullet\text{---}\bullet \rangle, \quad (22)$$

where the expectation value in this case corresponds to the full action and, working with an N -site d -dimensional lattice, the number of links and plaquettes is given by $N_l = Nd$, and $N_p = d(d-1)N/2$, respectively.

Disconnected contributions to these observables in the S_0 background are calculated in the manner introduced in Section 3, and elaborated further in Appendix A. The required expectation values, along with the associated multiplicities, of the relevant diagrams are also tabulated in Appendix A for reference. In order to present reasonably concise expressions we refer to the relevant connected contribution from diagram di as $C_i = m_i \langle D_i \rangle_C$ where m_i is the multiplicity and $\langle D_i \rangle_C$ is the connected expectation value obtained by subtracting the disconnected components from $\langle D_i \rangle_0$ in the standard manner.

We consider first the pure gauge sector of the theory. It is clear that in the limit $\beta_h \rightarrow 0$ the partition function reduces to that of pure $SU(2)$ gauge theory multiplied by an overall factor determined by the integration over the Higgs modulus, which factors out of expectation values. We now consider the average plaquette for non-zero β_h in the symmetric phase. To first order in δ the expectation value is given by

$$\langle E_P \rangle = \frac{1}{N_p} (\langle \square \rangle_0 + \delta \langle \square(S - S_0) \rangle_C + O(\delta^2)). \quad (23)$$

Recalling that only connected diagrams contribute, the contribution to $O(\delta)$ is given by

$$\langle E_P \rangle_1 = C_1 + \beta(C_6 + C_7) - JC_8. \quad (24)$$

The variational parameter must now be fixed by using the PMS criterion described earlier. Considering for a moment a general observable $\langle \mathcal{O}(\beta, \beta_h, \beta_r, J) \rangle$, the procedure used throughout is to examine $\langle \mathcal{O} \rangle$ at fixed β, β_h, β_r as a function of J , fixing the parameter at the ‘‘flattest’’ local extremum $J = \tilde{J}$ in accordance with PMS. As a result, the expectation value has the functional dependence $\langle \mathcal{O} \rangle = \langle \mathcal{O}(\beta, \beta_h, \beta_r, \tilde{J}(\beta, \beta_h, \beta_r)) \rangle$ and, due to

FIGURES

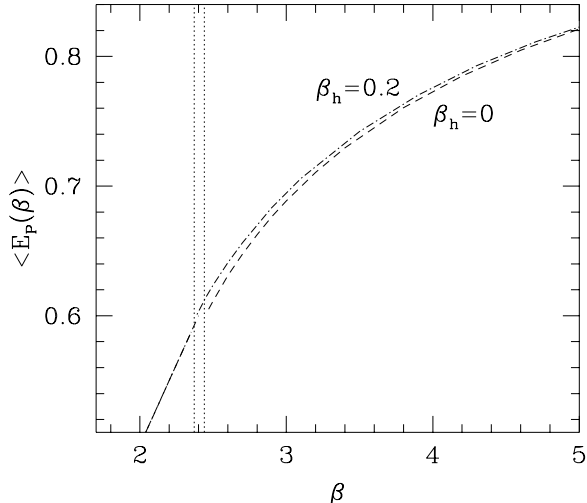


FIG. 1. The plaquette energy E_P as a function of β for $(\beta_h = 0, \beta_r = 0)$ and also $(\beta_h = 0.2, \beta_r = 0.5)$, a smooth transition between PMS branches occurring at $\beta \approx 2.44$ and 2.37 respectively.

discontinuous jumps between the PMS extrema \tilde{J} , may exhibit non-analyticities even when $\langle \mathcal{O}(\beta, \beta_h, \beta_r, J) \rangle$ is an analytic function of its parameters. Thus one associates the non-analyticity of discontinuous observables across a first order transition with jumps in the PMS solution \tilde{J} . Therefore the appearance or disappearance of a particular \tilde{J} as one moves over the parameter space is associated with a phase transition of the system if the resulting observable exhibits a discontinuity. This interpretation is justified by the experience with this technique in lattice gauge theory and in particular the study of the $SU(2) - SO(3)$ phase diagram [26], where the results agreed very well with the expectations from Monte Carlo simulations.

Returning now to the average plaquette expectation, we plot the results in Fig. 1 as a function of β for $\beta_h = 0$ (pure gauge theory) and $\beta_h = 0.2$ (well into the symmetric phase). One observes that the results are remarkably similar, indicating that the presence of the Higgs sector has little effect. This conclusion is consistent with explicit analysis of the $\langle E_P \rangle$ expectation values (see Appendix B), which suggests that the first Higgs sector corrections in the symmetric phase are generically of $O((\beta_h/2)^4)$.

The structure of the free action S_0 indicates that the limit $J = 0$ corresponds to the standard strong coupling expansion, and indeed a PMS solution exists for all β at $J = 0$. A second PMS solution first appears at $\beta \sim 2.4$, then flattens out to become the clear PMS point as β increases. This transition to a “weak coupling” branch occurs, however, at almost precisely the same value of $\langle E_P \rangle$, and with no distinctive change in behaviour, implying that the transition is actually a crossover. This deconfinement crossover is indeed consistent with expectations from lattice Monte Carlo studies in $4D$ [4,3,6], as is the slight shift of the crossover to lower values of β as β_h increases.

We now turn now to consideration of the hopping term which, for small Higgs masses, serves as a useful gauge invariant operator which is discontinuous across the first-order

transition. In order to analyse the behaviour as precisely as possible we take the calculation to $O(\delta^3)$,

$$\langle E_L \rangle = \frac{1}{N_l} \left(\sum_{n=0}^3 \frac{\delta^n}{n!} \langle \bullet\text{---}\bullet (S - S_0)^n \rangle_C + O(\delta^4) \right). \quad (25)$$

The relevant connected diagrams and their expectation values are enumerated in Appendix A. The result is given by

$$\begin{aligned} \langle E_L \rangle = & C_1 + \delta(2(d-1)\beta C_4 - J C_5) \\ & + \frac{\delta^2}{2} \left(\beta^2 \frac{d-1}{2} (C_{10} + C_{11} + C_{12}) - \beta J(d-1)(C_{13} + C_{14}) + J^2 C_{15} \right) \\ & + \frac{\delta^3}{6} \left(\beta^3 \frac{d-1}{2} \sum_{i=27}^{36} C_i - 3\beta^2 J \frac{d-1}{2} \sum_{i=37}^{43} C_i \right. \\ & \left. + 3\beta J^2 \frac{d-1}{2} (C_{44} + C_{45} + C_{46}) - J^3 C_{47} \right) + O(\delta^4). \end{aligned} \quad (26)$$

Considering first the expectation value at $O(\delta)$ only, we indeed find a transition between PMS branches in the region of $\beta_h \approx 0.31 - 0.38$ consistent with Monte Carlo expectations for the first-order transition. However, there is a region in parameter space in the transition region between these two branches for which no PMS extrema exist. This is not unexpected, as the expectation value undergoes a discontinuous shift. However, it does mean that a precise determination of the critical point will prove difficult working directly from $\langle E_L \rangle$. Analysing a range of β values, the results are presented in Fig. 2 for a 4D Higgs mass of 70 GeV, where this constraint determines β_r via (3) and (5). Since the approximation used in evaluating the integral over the Higgs modulus is expected to be most accurate in the $\beta \rightarrow 0$ limit, we restrict ourselves to relatively small values of β in this particular calculation.

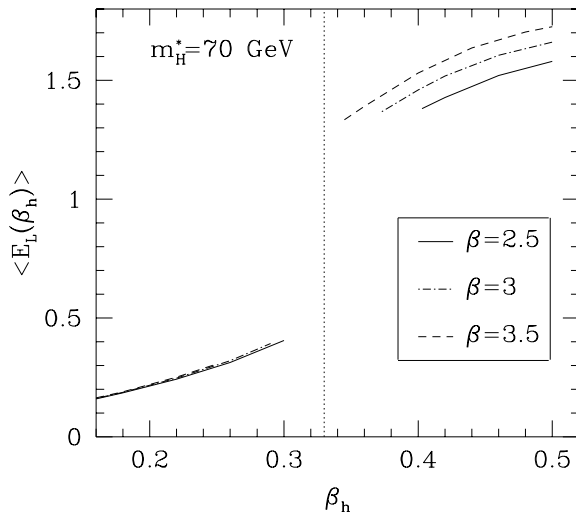


FIG. 2. We plot $\langle E_L \rangle_1$ versus β_h for a 4D Higgs mass $m_H^* = 70$ GeV, and three values of β . The vertical line is simply a rough guide to the position of the transition region $\beta_h = 0.31 - 0.35$.

The results presented in Fig. 2 are extended to $O(\delta^3)$ in Fig. 3. One observes that the transition region is now more clearly defined, with the PMS branches persisting closer to the transition point itself. At this order one has additional Higgs terms from diagrams at $O(\delta^0)$ ($d1$), and $O(\delta^1)$ ($d4$ and $d5$), correcting the slowly varying Higgs approximation in the evaluation of A_r^n . However, we note that in the transition region the behaviour of $\langle E_L \rangle$ is dominated by long wavelength modes, and thus the approximation used should be appropriate. A sample analytic calculation of the correction term is presented in Appendix B, and provided one assumes that the modulus of the Higgs field varies by no more than 10% over a lattice spacing, one finds that the correction terms are negligibly small when compared with the original contribution at the appropriate order in δ .

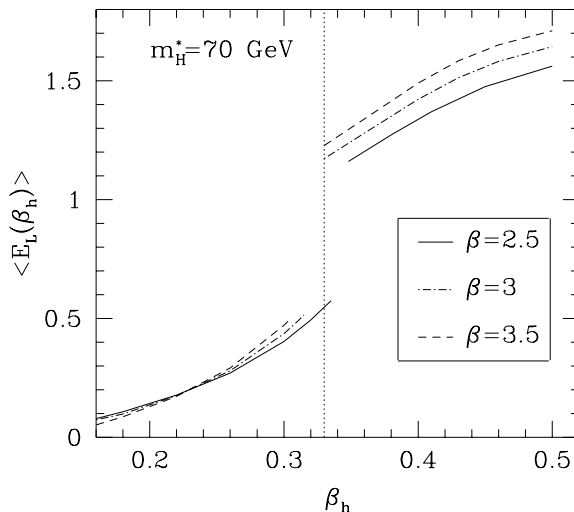


FIG. 3. We plot $\langle E_L \rangle_3$ versus β_h for a 4D Higgs mass $m_H^* = 70$ GeV, and three values of β . The vertical line is at the same value of β_h as in Fig. 2.

In order to determine the transition point more precisely, we now consider the second-order cumulant of E_L , defined by $C(E_L) \equiv \langle E_L^2 \rangle - \langle E_L \rangle^2$. To $O(\delta)$ this expectation may be represented as,

$$C(E_L) = \frac{1}{N_l} \langle \bullet \text{---} \bullet^2 \rangle_C \quad (27)$$

$$= C_{48} + \delta \left(\beta \frac{d-1}{2} (C_{49} + C_{50} + C_{51}) - J(C_{52} + C_{53}) \right) + O(\delta^2). \quad (28)$$

The cumulant exhibits a PMS solution for small β_h , but as β_h is increased this solution is lost at β_{hc} , above which no PMS extrema exist. Accordingly, we associate this point with the phase transition point. Tracking this line for increasing β we obtain an estimate for the transition line along the RG trajectories in the phase diagram for 4D Higgs masses of 60 and 70 GeV. The results are shown in Fig. 4 and compared with known Monte Carlo points in the diagram from the simulations presented in [31], [40], and Lee-Yang zeros analysis in [11]. Our procedure, even at this low order, produces close agreement with the Monte Carlo results.

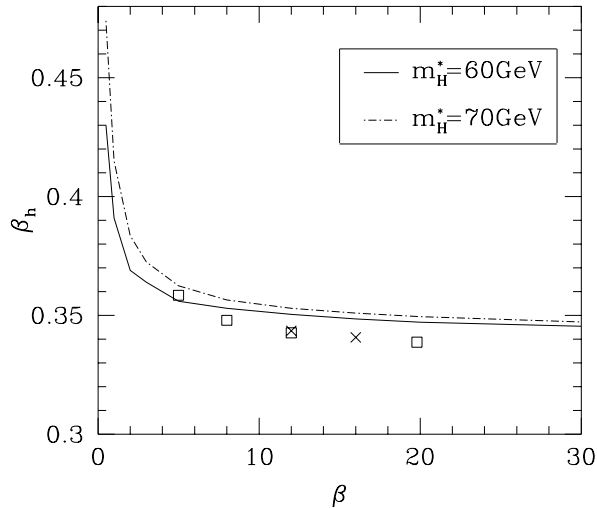


FIG. 4. We plot the critical curves in the (β_h, β) phase diagram for Higgs masses of 60 and 70 GeV. The critical values of β_h were determined to be those points at which a PMS extremum for the cumulant $C(E_L)_1$ was just lost; the values corresponding to a discontinuity of the cumulant. The results are compared with the Monte Carlo results of [31] (squares), and [40] and [11] (crosses) for $m_H^* = 60$ GeV.

Extrapolating to the continuum limit along the RG trajectory, we obtain critical couplings for each Higgs mass. Using (3) and (6) we can also determine the critical temperature and perform a similar extrapolation to the continuum. However, as one observes from Fig. 4, the continuum limit of β_{hc} is approximately 3% above the Monte Carlo estimates. Although this is entirely satisfactory for the order of the calculation, the sensitivity of the critical temperature to the value of β_{hc} results in estimates for the critical temperature being significantly lower than one would expect. In the low β region, however, where the results at this order are expected to be most accurate, the critical temperature agrees with Monte Carlo results [31] up to 20-25%. Note also that while the first-order cumulant appears to over-estimate the critical coupling β_{hc} , the transition region determined by analysis of $\langle E_L \rangle$ gives an under-estimate, for the relevant β range, of 6-8%. This discrepancy provides a reasonable estimate of the systematic errors of these results.

Increasing the Higgs mass beyond the regime where the first-order transition is expected to end, we find that the results change qualitatively only in the sharpness of the transition. In Fig. 5 the observable $\langle E_L \rangle_3$ is plotted at $\beta = 3$ for a 4D Higgs mass of 120 GeV. One observes that the PMS solutions do not persist as far into the transition region in comparison with the results at $m_H^* = 70$ GeV, and that the discontinuity itself is slightly smaller in magnitude. Although it is not possible from this result alone to characterise the transition as an analytic crossover rather than a first-order transition, it is certainly consistent with the former interpretation, which is suggested by previous studies.

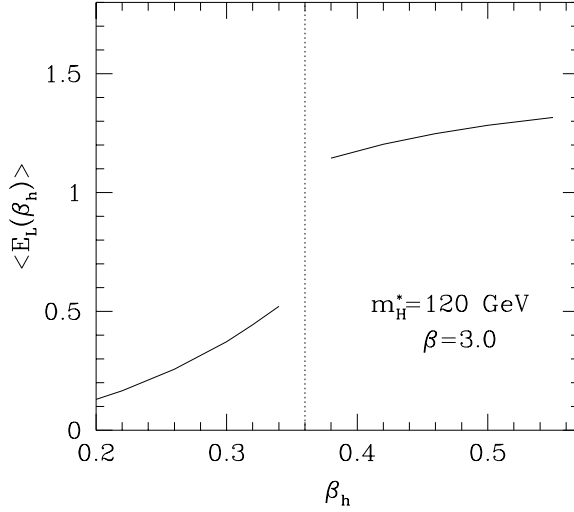


FIG. 5. We plot $\langle E_L \rangle_3$ versus β_h for a 4D Higgs mass $m_H^* = 120 \text{ GeV}$ at $\beta = 3$. The vertical line indicates the transition/crossover region.

The results are also consistent with the fact that Monte Carlo simulations indicate that the crossover is still extremely sharp for a Higgs mass in this region. Fig. 6, in which the calculation is repeated at $m_H^* = 140 \text{ GeV}$, shows a further reduction in the sharpness of the transition, as one observes from the increase in the parameter range for which no PMS solution exists.

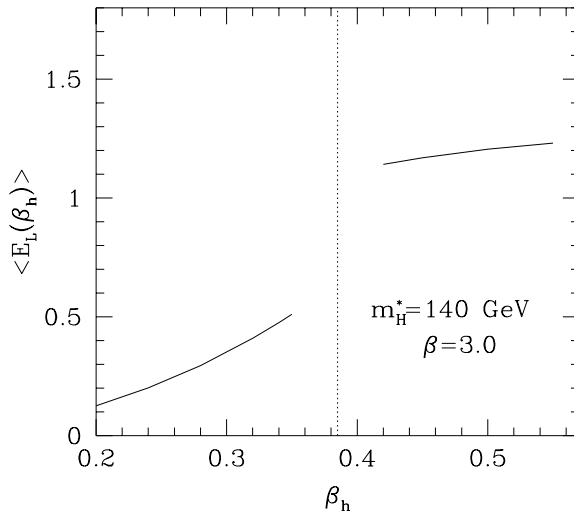


FIG. 6. We plot $\langle E_L \rangle_3$ versus β_h for a 4D Higgs mass $m_H^* = 140 \text{ GeV}$ at $\beta = 3$. The vertical line indicates the transition/crossover region.

Increasing the Higgs mass beyond $\sim 150 \text{ GeV}$ leads to a loss of the PMS solution in the broken phase. This is most likely to be a finite order effect with little direct relevance for the true phase structure, and for this reason we shall ignore such large Higgs masses. In studying

the second-order cumulant, we find that the qualitative behaviour is again unchanged until the Higgs mass becomes very large. In the region of interest, 80 – 120 GeV, the loss of a PMS solution at a critical value of β_h may presumably be associated with the sharpness of the crossover in this regime.

V. DISCUSSION

In this paper we have made use of a variant of the linear δ -expansion to examine the phase structure of the $SU(2)$ -Higgs model in $3D$. Using the previously derived matching conditions between the parameters of this model and a suitable approximation of the full $4D$ finite temperature electroweak theory we were able to extract the phase structure, consistent with lattice Monte Carlo simulations for small Higgs masses. Increasing the Higgs mass beyond the point where the first-order transition is expected to be replaced by a smooth crossover, the discontinuities in the observable $\langle E_L \rangle$ persist, but become less pronounced, as m_H^* increases. A higher order calculation in δ may be necessary in order to observe a more significant qualitative change in the behaviour of the relevant observables.

Nevertheless, this work does suggest a number of immediate extensions which are currently under consideration. The formalism developed here, in combination with the approach used in [30], allows an analytic study of the spectrum in the symmetric phase, in particular near the critical endpoint, where the lack of any finite volume restriction makes the regime dominated by large correlation lengths quite accessible without detailed finite volume scaling analysis. Recent work on the spectrum of the $3D$ theory for large Higgs masses suggests that in this respect the Higgs and confining phase have very similar properties [14].

The technique also suggests the possibility of studying the adjoint $SU(2)$ -Higgs model, as the dimensionally reduced effective theory for QCD [41–43]. A study of the phase structure of the mixed fundamental and adjoint $SU(2)$ gauge theory [26], which is the lowest order correction to pure $SU(2)$ gauge theory from a weak coupling expansion in β_h of the adjoint Higgs model [41], has already been successfully carried out using similar techniques.

However, given the remarkable level of precision that Monte Carlo techniques have been able to attain in this area, it is perhaps more appropriate to pursue the study of problems which are rather less accessible to such simulations. For instance, the possibility exists for studying the full $4D$ finite temperature theory directly [20]. Furthermore, study of the $U(1)$ -Higgs model, with the inclusion of a chemical potential in the context of superconductivity, appears feasible whereas, in contrast, the additional phase introduced by the chemical potential renders Monte Carlo simulations for this system very problematic.

ACKNOWLEDGEMENTS

The financial support of T.S.E by the Royal Society, and A.R. by the Commonwealth Scholarship Commission and the British Council, is gratefully acknowledged. This work was supported in part by the European Commission under the Human Capital and Mobility programme, contract number CHRX-CT94-0423.

APPENDIX A: CALCULATIONAL TECHNIQUES AND EXPECTATION VALUES

In this appendix we briefly discuss certain aspects of the techniques used for evaluation of the expectation values within the LDE. All the required expectations may be reduced to the form

$$\langle X \rangle_0 = \frac{1}{Z_0} \int [dU][d\rho] X e^{S_0}, \quad (\text{A1})$$

where in all cases X corresponds to a product of real constants, factors of ρ , and $SU(2)$ characters $\chi_r(U) = (\text{Tr}U)_r$. In addition S_0 , up to terms in ρ , also consists of fundamental $SU(2)$ characters. Thus the exponential may be represented as a character expansion

$$e^{\frac{1}{2}J\chi_{1/2}(U)} = \frac{2}{J} \sum_{r=0} I_{r+1}(J) \chi_{r/2}(U), \quad (\text{A2})$$

where $I_r(J)$ are modified Bessel functions.

Almost all the required expectation values X may be converted into simple character factors for each link using a combination of Clebsch-Gordan expansions, and the following relations, which follow easily using the invariance of the Haar measure and S_0 under a unitary transformation [19]:

$$\langle \chi_{r/2}(U^{2^n}) \rangle = (r+1)^{1-2^n} \langle \chi_{r/2}(U) \rangle^{2^n}. \quad (\text{A3})$$

Note that these relations also hold when there are additional single-link characters of U present in the expectation. With these techniques most of the required expectations are reduced to a product of constants and simple character factors. The group integration then becomes trivial via use of the orthogonality relation

$$\int [dU] \chi_r(UV) \chi_{r'}(U^{-1}W) = \frac{1}{\dim(r)} \delta^{rr'} \chi_r(VW). \quad (\text{A4})$$

The remaining integration over ρ may then be evaluated numerically using (17). As an example, consider evaluation of the following expectation value:

$$\langle D_4 \rangle_0 = \frac{1}{4} \left\langle \rho_1^2 \chi_{1/2}(U_1 U_2 U_3^\dagger U_4^\dagger) \chi_{1/2}(U_1) \right\rangle_0 \quad (\text{A5})$$

$$= \frac{1}{2^5} \left\langle \rho_1^2 \chi_{1/2}(U_2) \chi_{1/2}(U_3^\dagger) \chi_{1/2}(U_4^\dagger) (1 + \chi_1(U_1)) \right\rangle_0 \quad (\text{A6})$$


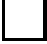







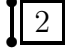





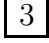
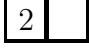

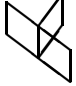

$$= \frac{1}{2^5} (B_1^0)^3 (B_0^1 + B_2^1). \quad (\text{A7})$$

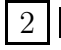


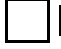
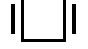

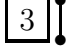
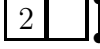
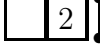
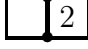

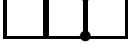
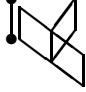
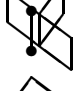
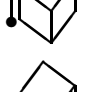
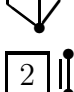
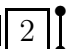

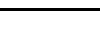
In the second line we have made use of (A3), and a Clebsch-Gordan expansion for $(\chi_{1/2}(U))^2$.

However, there are certain diagrams appearing at third order in δ which cannot be reduced to simple character factors for each link due to the degree of connectedness of the plaquettes. For example, see diagrams d20, d35 and d36. In order to calculate the required expectations in this case we use the projection operator technique elaborated in

the Appendix of [30], which allows the direct evaluation of un-traced products of a single link. We refer the reader to [30] for more details.

For each diagram required for the analysis in Section 4 the disconnected expectation values ($\langle D_i \rangle$) calculated in the manner described above, and also the corresponding multiplicities (m_i), are now presented in the following table. For convenience we define the constants $d_1 = 2d - 3$, $d_2 = 2d - 4$, $d_3 = d - 1$, and $d_4 = 2d - 1$.

$d\#$	D_i	m_i	$\langle D_i \rangle_0$
d1		1	$\frac{1}{2}B_1^1$
d2		1	$\frac{1}{16}(B_1^0)^4$
d3		1	$\frac{1}{2}B_1^0$
d4		4	$\frac{1}{32}(B_0^1)^3(B_0^1 + B_2^1)$
d5		1	$\frac{1}{4}(B_0^1 + B_2^1)$
d6		1	$\frac{1}{4}(1 + \frac{1}{27}(B_2^0)^4)$
d7		$4d_1$	$\frac{1}{256}(B_1^0)^6(1 + B_2^0)$
d8		4	$\frac{1}{4}(1 + \frac{1}{27}(B_2^0)^4)$
d9		1	$\frac{1}{4}(1 + B_2^0)$
d10		4	$\frac{1}{8}B_1^1 + \frac{1}{216}(B_2^0)^3(B_1^1 + B_3^1)$
d11		$24d_1$	$\frac{1}{512}(B_0^1)^5(1 + B_2^0)(B_0^1 + B_2^1)$
d12		$4d_1$	$\frac{1}{512}(B_0^1)^6(2B_1^1 + B_3^1)$
d13		4	$\frac{1}{64}(B_0^1)^3(2B_1^1 + B_3^1)$
d14		12	$\frac{1}{64}(B_0^1)^2(1 + B_2^0)(B_0^1 + B_2^1)$
d15		1	$\frac{1}{8}(2B_1^1 + B_3^1)$
d16		1	$\frac{1}{32}((B_1^0)^4 + \frac{1}{16}(B_3^0)^4)$
d17		$12d_1$	$\frac{1}{26}(1 + \frac{1}{33}(B_0^1)^3(B_2^0)^3(B_1^0 + B_3^0))$
d18		$36d_1^2 - 24d_2$	$\frac{1}{212}(B_1^0)^8(1 + B_2^0)^2$
d19		$4d_1d_2$	$\frac{1}{212}(B_1^0)^9(2B_1^0 + B_3^0)$
d20		$8d_2$	$\frac{1}{3^2 2^{10}}(B_1^0)^6(2(B_2^0)^3 + 9(B_2^0)^2 + 9)$

$d\#$	D_i	m_i	$\langle D_i \rangle_0$
d21		4	$\frac{1}{8}(B_1^0 + \frac{1}{3^3}(B_2^0)^3(B_1^0 + B_3^0))$
d22		$24d_1$	$\frac{1}{2^9}(B_1^0)^5(1 + B_2^0)^2$
d23		$4d_1$	$\frac{1}{2^9}(B_1^0)^6(2B_1^0 + B_3^0)$
d24		4	$\frac{1}{2^6}(B_1^0)^3(2B_1^0 + B_3^0)$
d25		12	$\frac{1}{2^6}(B_1^0)^2(1 + B_2^0)^2$
d26		1	$\frac{1}{8}(2B_1^0 + B_3^0)$
d27		4	$\frac{1}{64}(B_1^0)^3(B_0^1 + B_2^1) + \frac{1}{2^{10}}(B_3^0)^3(B_2^1 + B_4^1)$
d28		$36d_1$	$\frac{1}{2^7}(B_1^0)^2(B_0^1 + B_2^1)(B_1^0 + \frac{1}{3^3}(B_2^0)^3(B_1^0 + B_3^0))$
d29		$36d_1$	$\frac{1}{2^7}(B_1^0)^3(B_0^1 B_1^1 + \frac{1}{3^3}(B_2^0)^2(B_1^0 + B_3^0)(B_1^1 + B_3^1))$
d30		$12d_1$	$\frac{1}{2^7}(B_1^0)^3(B_0^1 + B_2^1 + \frac{1}{3^3}(B_2^0)^3(B_0^1 + 2B_2^1 + B_4^1))$
d31		$288d_1^2 - 192d_2$	$\frac{1}{2^{13}}(B_1^0)^7(1 + B_2^0)^2(B_0^1 + B_2^1)$
d32		$72d_1^2 - 48d_2$	$\frac{1}{2^{13}}(B_1^0)^8(1 + B_2^0)(2B_1^1 + B_3^1)$
d33		$36d_1 d_2$	$\frac{1}{2^{13}}(B_1^0)^8(B_0^1 + B_2^1)(2B_1^0 + B_3^0)$
d34		$4d_1 d_2$	$\frac{1}{2^{13}}(B_1^0)^9(2B_0^1 + 3B_2^1 + B_4^1)$
d35		$48d_2$	$\frac{1}{3^2 2^{10}}(B_1^0)^5(B_0^1 + B_2^1)(2(B_2^0)^3 + 9(B_2^0)^2 + 9)$
d36		$24d_2$	$\frac{1}{3^2 2^{12}}(B_1^0)^6(4B_2^0 B_3^1(B_2^0 + 3) + 2B_1^1(5(B_2^0)^2 + 6B_2^0 + 9))$
d37		4	$\frac{1}{16}(B_0^1 + B_2^1 + \frac{1}{3^3}(B_2^0)^3(B_0^1 + 2B_2^1 + B_4^1))$
d38		12	$\frac{1}{16}(B_0^1 B_1^0 + \frac{1}{3^3}(B_2^0)^2(B_1^0 + B_3^0)(B_1^1 + B_3^1))$
d39		$24d_1$	$\frac{1}{2^{10}}(B_1^0)^5(1 + B_2^0)(2B_1^1 + B_3^1)$

$d\#$	D_i	m_i	$\langle D_i \rangle_0$
d40		$24d_1$	$\frac{1}{2^{10}}(B_1^0)^5(2B_1^0 + B_3^0)(B_0^1 + B_2^1)$
d41		$24d_1$	$\frac{1}{2^{10}}(B_1^0)^5(2B_1^1 + B_3^1)(1 + B_2^0)$
d42		$4d_1$	$\frac{1}{2^{10}}(B_1^0)^6(2B_0^1 + 3B_2^1 + B_4^1)$
d43		$120d_1$	$\frac{1}{2^{10}}(B_1^0)^4(1 + B_2^0)^2(B_0^1 + B_2^1)$
d44		4	$\frac{1}{2^7}(B_1^0)^3(2B_0^1 + 3B_2^1 + B_4^1)$
d45		24	$\frac{1}{2^7}(B_1^0)^2(2B_1^1 + B_3^1)(1 + B_2^0)$
d46		24	$\frac{1}{2^7}B_1^0(2B_0^1 + B_2^1)(1 + B_2^0)^2$
d47		1	$\frac{1}{16}(2B_0^1 + 3B_2^1 + B_4^1)$
d48		1	$\frac{1}{4}(B_0^2 + B_2^2)$
d49		4	$\frac{1}{2^6}(B_1^0)^3(2B_1^2 + B_3^2)$
d50		8	$\frac{1}{2^6}(B_1^0)^2(B_0^1 + B_2^1)^2$
d51		$32d_3$	$\frac{1}{2^6}(B_1^0)^3B_1^1(B_0^1 + B_2^1)$
d52		1	$\frac{1}{8}(2B_1^2 + B_3^2)$
d53		$4d_4$	$\frac{1}{8}B_1^1(B_0^1 + B_2^1)$

APPENDIX B: EXPANSION OF A_R^N , AND HIGHER ORDER CORRECTIONS

After the group integrations have been performed, all expectation values up to $O(\delta^2)$ reduce to a series of ratios of the integral (17),

$$(A_r^n)^d = \int_0^\infty d\rho \rho^{2n+3} e^{-V_H} \left((r+1) \frac{I_{r+1}(J + \beta_h \rho^2)}{\frac{1}{2}(J + \beta_h \rho^2)} \right)^d, \quad (\text{B1})$$

for various choices of n and r depending on the diagram being evaluated. While the integral may easily be performed numerically, it is useful to consider an analytic series solution, particularly in the strong coupling regime $\beta \rightarrow 0$, and in the regime of a minimal gauge-Higgs coupling, $\beta_h \ll 1$.

As was discussed in Section 4, the LDE approach naturally includes a solution at $\tilde{J} = 0$ which corresponds to the strong coupling expansion appropriate for $\beta \ll 1$. We now wish to express (B1) as an expansion in β_h . Expanding the modified Bessel function in a power series, we may represent the integral in the form

$$(A_r^n)^d = \int_0^\infty d\rho \rho^{2n+3} e^{-V_H} \left[\sum_{k=0}^\infty \lambda_k \right]^d \quad (\text{B2})$$

$$= \int_0^\infty d\rho \rho^{2n+3} e^{-V_H} \sum_{m=0}^\infty c_m \quad (\text{B3})$$

where

$$\lambda_k = \frac{r+1}{k!(k+r+1)!} \left(\frac{J + \beta_h \rho^2}{2} \right)^{r+2k}, \quad (\text{B4})$$

and in (B3) we have expressed the d^{th} power of the series in λ_k as a new series with terms c_m which satisfy the recursion relation,

$$c_m = \frac{1}{m\lambda_0} \sum_{p=1}^m (pd - m + p) \lambda_p c_{m-p}, \quad (\text{B5})$$

with initial condition $c_0 = \lambda_0^d$. This recursion relation may be solved by noting that the structure implies that c_m is given by a sum of products of the λ_k whose exponents in each monomial are given by an appropriate partition of m . The structure of the coefficients of these monomials is then easily deduced, and one finds that the terms c_m have the general form

$$c_m = \sum_{\{i_p\}}^{\sum_{p=1}^m p i_p = m} \frac{d!}{\prod_{p=1}^m i_p! (d - \sum_{p=1}^m i_p)!} \lambda_0^{d - \sum_{p=1}^m i_p} \prod_{p=1}^m \lambda_p^{i_p}. \quad (\text{B6})$$

In the strong coupling limit with $J = 0$ one may then readily perform the integration over ρ to obtain A_r^n as a power series in β_h . In the general case, after forming the product of the factors $\lambda_p^{i_p}$ in (B6), we expand λ_k in (B4) as a power series in β_h , giving c_m as an explicit power series in β_h . For compactness in the following results we define $\sigma_t \equiv \sum_{q=1}^m (q)^t i_q$, where

the i_q are determined by the relevant partition of m . With this definition, the result for c_m becomes

$$c_m = \sum_{\{i_p|\sigma_1=m\}} P(d, m, r) \left(\frac{J}{2}\right)^{rd+2\sigma_1} \sum_{s=0}^{rd+2\sigma_1} \left(\frac{rd+2\sigma_1}{s}\right) \left(\frac{\beta_h}{J}\right)^s \rho^{2s}, \quad (\text{B7})$$

where

$$P(d, m, r) \equiv \frac{d!(r+1)^{\sigma_0}}{(r!)^{d-\sigma_0} (d-\sigma_0)! \prod_{t=1}^m i_t! (t!(t+r+1)!)^{i_t}}. \quad (\text{B8})$$

Returning to the full integral, the ρ integration may now be performed using the relation

$$\int_0^\infty d\rho \rho^{2x+3} e^{-V_H(\beta_r)} = \frac{1}{2} (x+1)! C(\beta_r, 2x), \quad (\text{B9})$$

where C may be written in terms of a parabolic cylinder function $D_n(x)$ as

$$C(\beta_r, x) = e^{\frac{(1-2\beta_r)^2}{8\beta_r} - \beta_r} (2\beta_r)^{-1-\frac{x}{4}} D_{-\frac{x}{2}-2} \left(\frac{1-2\beta_r}{\sqrt{2\beta_r}} \right), \quad (\text{B10})$$

which tends to unity as $\beta_r \rightarrow 0$. Finally, the full integral is given by the power series

$$(A_r^n)^d = \sum_{m=0}^{\infty} \sum_{\{i_p|\sigma_1=m\}} P(d, m, r) \left(\frac{J}{2}\right)^{rd+2\sigma_1} \times \frac{1}{2} \sum_{s=0}^{rd+2\sigma_1} \left(\frac{rd+2\sigma_1}{s}\right) \left(\frac{\beta_h}{J}\right)^s Q(\beta_r, 2n+2s), \quad (\text{B11})$$

where $Q(\beta_r, 2x) = (x+1)! C(\beta_r, 2x)/2$. In the strong coupling limit ($J=0$) this reduces to

$$(A_r^n)_S^d = \sum_{m=0}^{\infty} \sum_{\{i_p|\sigma_1=m\}} P(d, m, r) \left(\frac{\beta_h}{2}\right)^{rd+2\sigma_1} Q(\beta_r, 2n+rd+2\sigma_1) \quad (\text{B12})$$

The lowest order terms of this expansion are given by

$$(A_r^n)_S^d = \left(\frac{\beta_h}{2}\right)^{rd} \frac{(n+rd/2+1)!}{2(r!)^d} \left[1 + \left(\frac{\beta_h}{2}\right)^2 d \frac{r(r+1)}{(r+2)!} (n+rd/2+2) + O\left(\frac{\beta_h}{2}\right)^4 \right]. \quad (\text{B13})$$

Thus, if we focus attention on the gauge sector and the lowest order contribution to the average plaquette energy, given by d^2 , we find that in the strong coupling region the β_h dependence is given by

$$B_1^0 = \frac{\beta_h}{2} \left(\frac{3}{4}\sqrt{\pi}\right)^{1/3} \left[1 + \frac{3}{2} \left(\frac{\beta_h}{2}\right)^2 + O\left(\frac{\beta_h}{2}\right)^4 \right]. \quad (\text{B14})$$

Therefore, according to the expectation value $\langle D_2 \rangle$, in this regime the leading dependence on β_h has the form $(\beta_h/2)^4$, which is a small correction throughout the symmetric phase where $\beta_h < 0.34$, a result which is borne out by the numerical analysis presented in Fig. 1.

While the previous results are exact for expectation values up to $O(\delta^2)$, our restriction of the Higgs modulus in the interaction to the form $\rho_i\rho_j = \rho_i^2 + \delta^2\rho_i\Delta\rho_i$ implies that higher order calculations of observables will require additional correction terms for the lower order diagrams. As we have worked only to $O(\delta^3)$, it is only necessary to consider the first-order correction to the $O(\delta^0)$ and $O(\delta)$ contributions to $\langle E_L \rangle$.

Calculation of the correction is conveniently illustrated in the case of Z_0 . Expanding the exponential correction term we obtain,

$$Z_0 = \int [\tilde{d}\rho] \prod_{l_{ij}} \int [dU_{ij}] e^{\frac{1}{2}(J + \beta_h \rho_i^2) \chi_{1/2}(U_{ij})} \sum_{n=0}^{\infty} \frac{\delta^{2n}}{2^n n!} (\rho_i \rho_j - \rho_i^2)^n (\chi_{1/2}(U_{ij}))^n, \quad (\text{B15})$$

where we define $[\tilde{d}\rho] = \prod_i d\rho_i \rho_i^3 \exp(-V_H)$. On performing a character expansion of the exponential, Z_0 may be expressed in the form

$$Z_0 = \int [\tilde{d}\rho] \prod_{l_{ij}} \sum_{n=0}^{\infty} \sum_{r \in \mathbf{Z}_+} (r+1) \frac{I_{r+1}(J + \beta_h \rho_i^2)}{\frac{1}{2}(J + \beta_h \rho_i^2)} \frac{\delta^{2n}}{2^n n!} (\rho_i \rho_j - \rho_i^2)^n \int [dU_{ij}] \chi_{r/2} \sum_{j=0,1/2}^{n/2} c_j \chi_j. \quad (\text{B16})$$

The final sum begins with $j = 0$ ($j = 1/2$) for even (odd) n , and the coefficients c_j are determined by the expansion of the product $(\chi_{1/2}(U_{ij}))^n$. This result is quite general and includes all higher order corrections. As mentioned earlier, we only require the first-order correction in the present case, corresponding to $n = 1$. To this order we have

$$Z_0 = \int [\tilde{d}\rho] \prod_i \left(\frac{I_1(J + \beta_h \rho_i^2)}{\frac{1}{2}(J + \beta_h \rho_i^2)} \right)^d \prod_{l_{ij}} \left[1 + \delta^2 (\rho_i \rho_j - \rho_i^2) \frac{I_2(J + \beta_h \rho_i^2)}{I_1(J + \beta_h \rho_i^2)} \right] + O(\delta^4). \quad (\text{B17})$$

If we focus on the expression in square brackets, then since the ratio of Bessel functions has an upper bound of unity for large values of its argument, one observes that the term of $O(\delta^2)$ is indeed a small correction provided that $\rho_i \sim \rho_j$ for i and j nearest neighbour sites. If one makes the assumption that ρ_i and ρ_j differ by at most 10%, which seems reasonable for expectation values dominated by long wavelength modes, then one finds that the correction is almost negligible despite appearing to be of $O(10\%)$ in (B17). The reason is that, for non-zero β_r , the integral (B17) is dominated by contributions from the region $\rho < 10 - 15$ for which the ratio I_2/I_1 is small. Furthermore, the correction needs to be compared with the disconnected expectation value at the appropriate order in δ rather than directly with its zeroth order contribution. Once one does this the correction is indeed found to be small having negligible effect on the results, as was discussed in Section 4.

This result may be made more explicit by extracting terms up to $O(\delta^2)$ from the product, which take the form $1 + \delta^2 \sum_{\langle ij \rangle} (\rho_i \rho_j - \rho_i^2) I_2(x_i)/I_1(x_i)$, where $x_i \equiv J + \beta_h \rho_i^2$,

$$Z_0 = \tilde{Z}_0^{N_s} \left(1 + \frac{\delta^2}{\tilde{Z}_0^2} \sum_{\langle ij \rangle} \tilde{Z}_{l_{ij}} + O(\delta^4) \right). \quad (\text{B18})$$

The first factor is given by the standard zeroth-order contribution,

$$\tilde{Z}_0 = \int [\tilde{d}\rho_i] \left(\frac{I_1(J + \beta_h \rho_i^2)}{\frac{1}{2}(J + \beta_h \rho_i^2)} \right)^d, \quad (\text{B19})$$

while the $O(\delta^2)$ correction also contains a sum of contributions of the form

$$\tilde{Z}_{1_{ij}} = \int [d\tilde{\rho}_i d\tilde{\rho}_j] (\rho_i \rho_j - \rho_i^2) \prod_{p=i,j} \left(\frac{I_1(x_p)}{\frac{1}{2}x_p} \right)^d \frac{I_2(x_i)}{I_1(x_i)}. \quad (\text{B20})$$

A further reduction in the relative magnitude of the correction would then follow from possible cancellations of terms in the sum over the links of the lattice, as the factor $(\rho_i \rho_j - \rho_i^2)$ will vary in sign.

REFERENCES

- [1] K. Kajantie, M. Laine, K. Rummukainen, and M. Shaposhnikov, Nucl. Phys. B **458**, 90 (1996).
- [2] K. Kajantie, M. Laine, K. Rummukainen, and M. Shaposhnikov, Nucl. Phys. B **493**, 413 (1997).
- [3] H. G. Evertz, J. Jersák, and K. Kanaya, Nucl. Phys. B **285**, 229 (1987).
- [4] P. Damgaard and U. M. Heller, Nucl. Phys. B **294**, 253 (1987).
- [5] P. Damgaard and U. M. Heller, Nucl. Phys. B **304**, 63 (1988).
- [6] W. Bock *et al.*, Phys. Rev. D **41**, 2573 (1990).
- [7] F. Csikor *et al.*, Nucl. Phys. B **474**, 421 (1996).
- [8] Y. Aoki, Nucl. Phys. B (Proc. Suppl.) **53**, 609 (1997).
- [9] K. Kajantie, M. Laine, K. Rummukainen, and M. Shaposhnikov, Phys. Rev. Lett. **77**, 2887 (1996).
- [10] F. Karsch, T. Neuhaus, A. Patkós, and J. Rank, Nucl. Phys. B (Proc. Suppl.) **53**, 623 (1997).
- [11] M. Gürtler, E. Ilgenfritz, and A. Schiller, Preprint: hep-lat/9704013 (1997).
- [12] E. Fradkin and S. H. Shenker, Phys. Rev. D **19**, 3682 (1979).
- [13] O. Philipsen, M. Teper, and H. Wittig, Nucl. Phys. B **469**, 445 (1996).
- [14] O. Philipsen, M. Teper, and H. Wittig, Preprint: hep-lat/9709145 (1997).
- [15] M. Reuter and C. Wetterich, Nucl. Phys. B **408**, 91 (1993).
- [16] N. Tetradis, Nucl. Phys. B **488**, 92 (1997).
- [17] W. Buchmüller and O. Philipsen, Nucl. Phys. B **443**, 47 (1994).
- [18] T. S. Evans, H. F. Jones, and A. Ritz, hep-th/9707539, to appear in: Proceedings of Eotvos Conference in Science: Strong and Electroweak Matter (SEWM 97), Eger, Hungary, 21-25 May 1997 (1997).
- [19] X.-T. Zheng, Z. G. Tan, and J. Wang, Nucl. Phys. B **287**, 171 (1987).
- [20] C.-I. Tan and X.-T. Zheng, Phys. Rev. D **39**, 623 (1989).
- [21] A. Duncan and M. Moshe, Phys. Lett. B **215**, 352 (1988).
- [22] A. Duncan and H. F. Jones, Nucl. Phys. B **320**, 189 (1989).
- [23] I. R. C. Buckley and H. F. Jones, Phys. Rev. D **45**, 654 (1992).
- [24] I. R. C. Buckley and H. F. Jones, Phys. Rev. D **45**, 2073 (1992).
- [25] J. O. Akeyo and H. F. Jones, Phys. Rev. D **47**, 1668 (1993).
- [26] J. O. Akeyo and H. F. Jones, Z. Phys. C **58**, 629 (1993).
- [27] X.-T. Zheng and B.-S. Liu, Int. J. Mod. Phys. A **6**, 103 (1991).
- [28] J. M. Yang, J. Phys. G **17**, L143 (1991).
- [29] J. M. Yang, C. M. Wu, and P. Y. Zhao, J. Phys. G **18**, L1 (1992).
- [30] J. O. Akeyo, C. S. Parker, and H. F. Jones, Phys. Rev. D **51**, 1298 (1995).
- [31] K. Kajantie, M. Laine, K. Rummukainen, and M. Shaposhnikov, Nucl. Phys. B **466**, 189 (1996).
- [32] P. M. Stevenson, Phys. Rev. D **23**, 2916 (1981).
- [33] I. R. C. Buckley, A. Duncan, and H. F. Jones, Phys. Rev. D **47**, 2554 (1993).
- [34] A. Duncan and H. F. Jones, Phys. Rev. D **47**, 2560 (1993).
- [35] J. Fröhlich, G. Morchio, and F. Strocchi, Nucl. Phys. B **190**, 553 (1981).
- [36] F. Karsch, T. Neuhaus, A. Patkós, and J. Rank, Nucl. Phys. B **474**, 217 (1996).
- [37] W. Buchmüller and O. Philipsen, Phys. Lett. B **397**, 112 (1997).

- [38] I. G. Halliday, Rep. Prog. Phys. **47**, 987 (1984).
- [39] P. Damgaard and U. M. Heller, Phys. Lett. B **164**, 121 (1985).
- [40] M. Gürtler *et al.*, Nucl. Phys. B **483**, 383 (1997).
- [41] S. Nadkarni, Nucl. Phys. B **334**, 559 (1990).
- [42] K. Kajantie, M. Laine, K. Rummukainen, and M. Shaposhnikov, Preprint: hep-ph/9704416 (1997).
- [43] A. Hart, O. Philipsen, J. D. Stack, and M. Teper, Phys. Lett. B **396**, 217 (1997).